Interfacial Lateral Electrical Conductance on Lipid Monolayer: Dose-Dependent Converse Effect of Alcohols

Tadayoshi Yoshida,* Yasutaka Koga, and Hajime Minowa

Department of Applied Chemistry, Nagoya Institute of Technology, Showaku, Nagoya 466, Japan

Hiroshi Kamaya and Issaku Ueda*

Anesthesia 112A, DVA Medical Center, Salt Lake City, Utah 84148

Received: August 2, 1999; In Final Form: October 18, 1999

From the temperature dependence of the impedance dispersion in dipalmitoylphosphatidylcholine liposomes, we reported that halothane decreased the apparent activation energy of the lateral surface conductance of phospholipid vesicles (Yoshida et al. *Biochim. Biophys. Acta* **1990**, *1028*, 95; Yoshino et al. *Biochim. Biophys. Acta* **1992**, *1107*, 55). However, the presence of proton flow within the electrical double layer at the lipid−water interface has been a matter of controversy. The difference in interpretation on two-dimensional proton flow is focused on imperfection in the experimental procedure, in particular, change of the meniscus of water surface at the electrode and the trough caused by monolayer formation, which changes the effective surface area of the electrode, pH instability due to local CO_2 concentrations, polarization by the accumulation of ions on the electrode surface, and temperature instability. We designed a novel horizontal-plate electrode, totally immersed in water, to eliminate formation of meniscus. Together with elimination of CO_2 in a completely enclosed measuring system and careful temperature control, we obtained conclusive results on the existence of lateral surface electric conductance. Alcohols (ethanol, 1-propanol, and 1-butanol) increased the surface electrical conductance at low concentrations and decreased it at high concentrations that induce anesthesia. Similar electrical conductance may exist at protein surfaces among charged amino acid side chains.

Introduction

The importance of hydrogen bonds in forming biologically meaningful structures of proteins and lipid membranes is well established. Hydrogen bonding also contributes to the proton flow during signal transduction and energy transfer. We[1] proposed that actions of amphipathic molecules such as anesthetics and alcohols are directed to macromolecule−water interface. Anesthetics compete with interfacial water molecules. Utilizing proton nuclear magnetic resonance spectrometry, ^{1}H NMR, it was shown that anesthetics increased proton spin−spin relaxation time in water-in-oil reversed micelles, indicating release of surface-bound water.[2] Release of surface-bound water was further confirmed by the spin−lattice relaxation time of ^{2}H NMR.[3] The spin−lattice relaxation time of ^{2}H NMR relates directly to the motion of ^2H_2O molecules and has an advantage over ^{1}H NMR. Differential scanning calorimetry of hydrated phospholipid membranes at subzero temperatures[4] showed existence of water molecules that freeze at various subzero temperatures. Anesthetics released water molecules, which did not melt at 0 °C and bound to lipid membranes. Fourier transform infrared spectroscopy showed that anesthetics[5,6] and alcohols[7] broke hydrogen bonding between interfacial water and phospholipid membranes.

The release of surface-bound water molecules was accompanied by a decrease of surface charge density of adsorbed monolayer at the water−oil interface, estimated from the drop volume of an electrocapillary system.[8] Decrease of surface charge density and weakening of water−lipid interaction at the membrane surface are expected to affect the lateral electrical conductance parallel to the lipid membrane surface. Impedance dispersion in liposomes measures the lateral charge transfer of lipid membrane surfaces. From the temperature dependence of impedance dispersion, we showed that halothane decreased the activation energy of lateral conductance of dipalmitoylphosphatidylcholine (DPPC) vesicle membranes at temperatures above pretransition of the membrane.[9,10]

Kell[11] proposed that proton flow parallel to the membrane surface is coupled to the proton pump mechanism. There have been a few efforts to identify the proton flow parallel to the membrane surface. These include estimation of an unequal local distribution of protons,[12,13] and estimation of the increment of lateral electric conductance when surface monolayers are formed on water.[14−17] These studies indicated the presence of proton flow parallel to the lipid membranes, the character of which is different from proton flow in the bulk water phase.

There are reports that oppose the above concept. Nachliel and Gutman[18] and Gutman et al.[19] used computer-based calculation and experimental results on a laser-excited proton emitter trapped close to the lipid membrane. They disputed the existence of proton flow parallel to the membrane. Kasianowicz et al.[20] and Menger et al.[21] questioned the experimental procedures of the reports maintaining the presence of the membrane-associated proton flow,[14−17] and concluded that the results are experimental artifacts. However, the methods and experimental procedures used by Sakurai et al.[14,15] and Morgan et al.[16,17] were similar to those used by Menger et al.[21] and reached contrary results.

The cause of the difference in interpretation of experimental results on the two-dimensional proton flow appears to be focused

* To whom correspondence should be addressed.

10.1021/jp992715y CCC: $19.00
Published on Web 01/25/2000

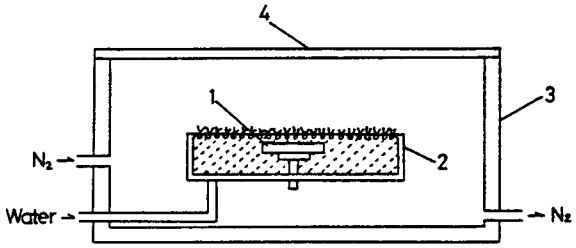

Figure 1. Block diagram of the structure of the isolation chamber to measure surface electrical conductance of spread monolayer under CO_2-free atmosphere: (1) horizontal electrode; (2) round trough to form spread monolayer; (3) enclosure of the measuring system by Teflon box (198 × 288 × 82 mm); (4) Pyrex glass plate.

on imperfection in the experimental procedure. The condition for obtaining reliable lateral electrical conductance is when lipid membranes are formed the stable baseline current in the absence of lipid monolayer must stay unchanged. Menger et al.[21] mentioned that the baseline current is affected by the change in (1) the regional distribution of the dissolved CO_2 concentration, (2) polarization of the electrodes by the accumulation of ions on the electrode surface, (3) the temperature of the water phase, and (4) meniscus formed at the electrode surface, which changes the effective electrode surface area. Because of these effects, baseline values may not be equal before and after monolayer formation. When the lipid is added to the water surface, spreading of lipid molecules at the water surface creates flow of water molecules below the monolayer which may also change the CO_2 distribution.

Theory and Procedure

To satisfy the above conditions, it is necessary to use a completely CO_2-free (N_2 saturated) system. The second problem can be solved by increasing the surface area of the electrode and using alternating current. However, the increase of the electrode surface increases baseline current. The surface conductance value becomes relatively smaller and makes the accurate measurement difficult. The third problem can be reduced to less than 0.05 °C by flowing temperature-controlled N_2 gas into the electrode chamber.

The fourth problem on the meniscus is the most difficult to solve. The formation of the monolayer decreases the surface tension of water and changes the shape of meniscus. The effective surface areas of the vertically placed pair of electrodes, employed by both Menger and Morgan, change because the electrodes cross the water surface. The baselines are not the same before and after the formation of the monolayer. The magnitude of the change depends on the size of the trough and electrodes, plus the materials and their surface properties (roughness, hydrophilicity, etc.). These problems may be the reason different research groups obtained varying experimental results, and also affected the reproducibility of the experimental values.

To solve these problems we devised a novel horizontal flat electrode with special attention to the shape of the trough. As shown in Figure 1, the horizontal electrode is immersed in water, eliminating formation of meniscus at the electrode. The edge of the trough is formed into a sharp angle. Maintaining the water surface to the trough edge, we successfully decreased the meniscus effect to be ignored. To eliminate the fluctuation in local pH by CO_2 absorption, we isolated the system from ambient air by enclosing the trough in a Teflon box and circulating CO_2-free constant-temperature N_2 gas. Utilizing these procedures, the problems are successfully eliminated.

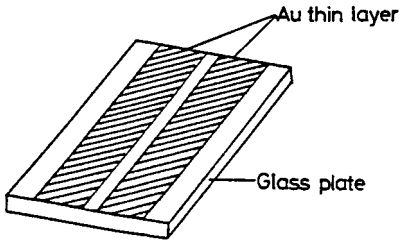

Figure 2. Horizontal electrode.The base board is Pyrex plate (50 × 60 × 5 mm). A pair of rectangular gold films (15 × 60 mm) with 4 mm distance are deposited by vacuum evaporation. The electrode plate is placed at 1 mm below the water surface.

Additionally, we paid special care to the surface contaminant molecules. The presence of surface contaminant affects the structure of the formed monolayer. To avoid surface contaminants, it was necessary to be careful about selecting the material to construct the apparatus. Plastics, glues, and adhesives contain surface-active volatile molecules. The presence of a small amount contaminates the surface due to condensation at the interface. Also, materials interfacing with water must be free of water-soluble material. The presence of stainless steel, copper, and other metallics affected experimental values. Our system was composed of Teflon, Pyrex glass, and gold. We used a minimum amount of copper and stainless steal for wires not touching water.

Under these conditions, the baseline current was stable for an extended time and was reproducible. The horizontal electrode was made of a Pyrex glass plate (8 mm thick × 50 mm × 60 mm) on the surface of which gold was deposited by a vacuum evaporation method. On the surface of the Pyrex glass, a pair of 15 × 60 mm rectangular gold thin films were placed 4 mm apart in parallel (Figure 2). The electrode was immersed in water, 1 mm below and parallel to the surface, in a round Teflon trough (140 mm diameter).

The Teflon trough was placed in a Teflon box (198 × 288 × 83 mm) tightly covered with a 5 mm thick Pyrex glass plate and filled with N_2 gas. The N_2 gas was fed through a gas-washing bottle and another glass bottle placed in a constant temperature water bath maintained at 25 °C. The gas flow rate was monitored by a digital flow meter (SEF-2 1A, Iuchi, Tokyo) and maintained at 500 mL min^{-1}. Purified water was obtained by a super water-purifying system (Pureline WL-21P, Yamato, Tokyo), with purity better than 0.07 μS cm^{-1}, and then boiled in a greaseless Pyrex glass flask for 15 min under N_2 gas to eliminate CO_2, and then cooled. The CO_2-free water was transferred to a Pyrex glass bottle, placed in a constant temperature water bath maintained at 25 °C, and then transferred into the monolayer-forming trough. To avoid contamination by air during these transfers, procedures were performed through Teflon tubes with Teflon stopcocks under N_2 gas. The electrical conductance between the two thin gold electrodes were measured by a digital conductance meter (CM-11P, Toa, Tokyo) at a frequency of 80 Hz.

Monolayers were formed with dipalmitoyl-L-α-phosphatidic acid (DPPA) (Sigma). DPPA was dissolved in benzene (Wako, Osaka) and applied on the water surface with a microsyringe (50 μL) through a small hole (1 mm diameter) in the cover. After the monolayer formation, the hole was closed by a Teflon block.

After the electrical conductance was stabilized, water solution of 1-alkanols (Wako, Tokyo), ethanol (better than 99.5%), 1-propanol (better than 99.8%), and 1-butanol (better than 99.0%) were slowly added to the water phase by a microsyringe.

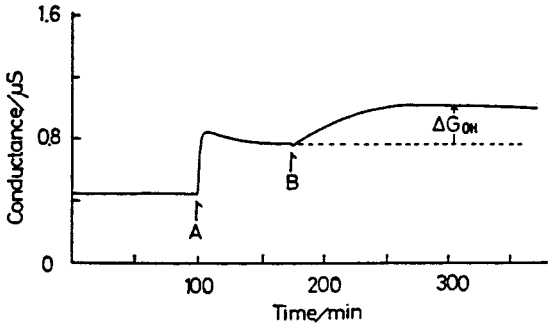

Figure 3. Time-dependent change in the electrical conductance. (A) Formation of lipid monolayer on a clean water surface in CO_2-free condition. Aliquot of 27 μL of 2.5 mM DPPA in benzene is applied to the water surface by a microsyringe. (B) Using a microsyringe, 100 μL of aqueous solution of 1.3 M 1-propanol was applied to the water surface. ΔG_{OH} is the difference in the electrical conductance before and after application of 1-propanol.

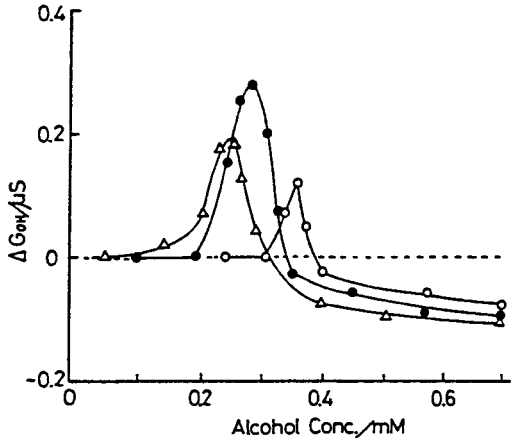

Figure 4. Dependence of surface electrical conductance on the alkanol concentration. Abscissa is the aqueous concentration of alkanols in millimoles, assuming homogeneous solvation. Open circles are for ethanol, closed circles are for 1-propanol, and open triangles are for 1-butanol.

Results and Discussion

Electrical conductances varied by the applied amount of DPPA dissolved in benzene. When 27 μL of 2.5 mM DPPA solution was applied to the surface, the surface area of one DPPA molecule was 0.50 nm^2 at 25 °C. An increase of DPPA solution increased the electrical conductance. When the area per DPPA molecule is decreased below 0.70 nm^2, the electrical conductance suddenly increased and showed a maximum at 0.50 nm^2. At this condition, the surface pressure was 46 mN m^{-1}. When the applied amount of the 2.5 mM DPPA solution exceeded 27 μL, formation of lenses was observed. Therefore, under the present experimental condition (0.50 nm^2 per DPPA molecule), the monolayer was close to the maximum packing. However, the occupied area is 20% larger than the maximum packing of two all-trans hydrocarbon tails, which is 40 nm^2.

Figure 3 shows the time-dependent change of electrical conductance in response to the addition of 1-propanol, observed by the horizontal flat electrode. After confirming the stability of baseline conductance, 27 μL of 2.5 mM DPPA−benzene solution was added to the water surface by a microsyringe at point A. Electrical conductance increased promptly, followed by a slow decrease with evaporation of benzene. After 60 min, conductance became stable. We assume the monolayer was formed on the water surface. At point B, a 100 μL aqueous solution of 1.3 M 1-propanol was added by a microsyringe. In time, the electrical conductance slowly changed and, in about 150 min, reached a steady state. The 1-propanol concentration in the aqueous phase was 0.30 mM. AT this time, interaction of added 1-propanol with the DPPA monolayer appeared to be completed, reaching a steady state. Figure 4 shows the difference of the electrical conductance, ΔG_{OH}, before and after the addition of 1-propanol.

Addition of the same amount (100 μL) of water did not affect the electrical conductance. In the absence of DPPA monolayer, addition of 1-propanol did not change the electrical conductance, $\Delta G_{OH} = 0$. Therefore, the dependence of ΔG_{OH} to 1-propanol was not produced by a change in the water level of the trough or the conductivity of added 1-propanol. The dependence of ΔG_{OH} on the concentration of 1-propanol is a result of direct interaction between DPPA monolayer and 1-propanol.

It has been established[7,22] that alcohols interact with the phosphate moiety of DPPC. Short-chain alcohols prefer to interact with the hydrophilic polar region rather than the hydrophobic hydrocarbon interior. From the change in line width of the ^{1}H NMR signal, it has been shown anesthetics induce the gel-to-liquid crystal transition of lipid bilayers and increase the mobility of the hydrophilic part of lipid bilayers.[23,24]

The assembly of lipid membranes cannot be formed without water. This indicates the importance of a hydrogen-bond network among the water molecules that contact with the hydrophilic moieties of the membrane. These water molecules function as adhesive between the amphipathic phospholipid molecules, maintaining the stability of the membrane by suppressing its fluidity.

When alcohol molecules interact with hydrophilic parts of the membrane, the hydrogen-bond network will be partially destroyed. The averaged area of 0.50 nm^2 per DPPA molecule indicates that phosphate moieties do not directly attach to the next neighbor DPPA. Several water molecules are present between phosphate moieties. These water molecules hinder the direct contact between next neighbor phosphate moieties, and the hydrogen bondings among water molecules suppress the movement of the phosphate moieties. Addition of alcohols breaks the hydrogen bonds and increases the motion of phosphate moieties. The increased motion (fluidization of lipid membrane) enhances the probability of colliding of phosphate moieties. Accordingly, the probability of proton transfer among phosphate moieties increases, resulting in the increase of surface electrical conductance. Therefore, alcohols are able to increase the surface electrical conductance. DPPA is a monoester and highly probable to function as a proton donor−acceptor pair.

In addition to the above mechanism of the proton transfer among the phosphate moieties, there is another possibility. This mechanism involves indirect proton transfer through the hydrogen bonds among water molecules in the hydration networks at the membrane−water interface. In this mechanism, alcohols disturb the hydration shell at the interface, inhibit the proton transfer, and decrease (inhibit) the indirect proton transfer. The short-chain alcohols, presently used, condense at the water−lipid interface, rather than penetrating into the hydrocarbon core. To the limit of short-chain alcohols, an increase of the hydrocarbon chain increases hydrophobicity and increases interfacial concentration of short-chain alcohols. Hence, it is possible, alcohols will decrease the surface electrical conductance as well. The increase of hydrocarbon chain increases alcohol concentration at the interfacial region. When evaluated by the aqueous concentrations, butanol increased electrical conductances more than ethanol by increasing the motion of phosphate moieties.

Figure 4 shows that ΔG_{OH} increased to a maximum and then decreased as the concentrations of all three alcohols were increased. Alcohols break hydrogen bonds, increase the probability of colliding of phosphate moieties, and enhance the proton transfer. On the other hand, the breaking of the hydrogen bonds weakens the hydrogen-bond network and suppresses the proton movements through the network. The cause of formation of the maximum by the increase of the alcohol chain length may be the combination of the two opposing effects.

Figure 4 also shows that longer-carbon-chain alcohols increased electrical conductance at lower concentrations. The partition coefficients of alcohols between bilayer membranes (DPPC vesicles) and water increased according to an increase in carbon-chain length: ethanol 2.53; 1-propanol 19.0; and 1-butanol 61.6.[25,26] Prolongation of the carbon-chain length of alcohols enhances the alcohol interaction with lipid membranes. As a result, longer-chain alcohols increase membrane fluidity and surface electrical conductance at lower concentrations.

The concentration of alcohols that showed maxima in electrical conductivity was in the range of 0.3 mM, and is much below the concentrations that induce anesthesia, which is in the range of 190 mM for ethanol in tadpoles. At clinical concentrations, the sign of ΔG_{OH} is negative. At present, the link between surface electrical conductance and the anesthesia mechanism is unclear. However, according to the hypothesis proposed by Kell,[11] the following paradigm may be possible. When the alcohol concentration exceeds a limiting value, the surface electrical conductance is suppressed (ΔG_{OH} becomes negative). This will decrease the proton flow of the proton pump incorporated into excitable cell membranes. The electrical conductance parallel to the membrane surface is controlled by (1) average distance between the next neighbor polar moieties, (2) fluidity of the membrane, and (3) hydrogen bond network. As a combined effect, alcohols decrease the proton flow and induce anesthesia.

This probably has relevance to the bimodal biological action of alcohols: stimulation at lower concentrations and inhibition at higher concentrations. The stimulatory action of alcohols at lower concentrations agrees with the excitation often complicating anesthesia at the start or during emergence from anesthesia when their concentrations are low. Electrical conductances through ion channels may follow a similar lateral conductance mechanism through the hydrogen-bond network of interfacial water molecules formed among charged amino acid side chains at the protein−water interface.

Acknowledgment. This study was supported in part by DVA Medical Research and Development Funds.

References and Notes

(1) Kamaya, H.; Ueda, I.; Eyring, H. In *Molecular Mechanisms of Anesthesia. Progress in Anesthesiology*; Fink, B. R., Ed.; Raven Press: New York, 1980; Vol. 2, p 429.

(2) Yoshida, T.; Okabayashi, H.; Takahashi, K.; Ueda, I. *Biochim. Biophys. Acta* **1984**, *772*, 102.

(3) Yoshino, A.; Yoshida, T.; Takahashi, K.; Ueda, I. *J. Colloid Interface Sci*. **1989**, *133*, 390.

(4) Ueda, I.; Tseng, H. S.; Kaminoh, Y.; Ma, S. M.; Kamaya, H.; Lin, S. H. *Mol. Pharmacol*. **1986**, *29*, 582−588.

(5) Tsai, Y. S.; Ma, S. M.; Kamaya, H.; Ueda, I. *Mol. Pharmacol*. **1987**, *31*, 623.

(6) Tsai, Y. S.; Ma, S. M.; Nishimura, S.; Ueda, I. *Biochim. Biophys. Acta* **1990**, *1022*, 245.

(7) Chiou, J. S.; Kuo, C. C.; Lin, S. H.; Kamaya, H.; Ueda, I. *Alcohol* **1991**, *8*, 143.

(8) Yoshida, T.; Okabayashi, H.; Kamaya, H.; Ueda. I. *J. Pharm. Sci.* **1991**, *80*, 852.

(9) Yoshida, T.; Taga, K.; Okabayashi,; H. Kamaya, H.; Ueda, I. *Biochim. Biophys. Acta* **1990**, *1028*, 95.

(10) Yoshino, A.; Yoshida, T.; Okabayashi, H.; Kamaya, H.; Ueda, I. *Biochim. Biophys. Acta* **1992**, 1107.

(11) Kell, D. B. *Biochim. Biophys. Acta* **1979**, *549*, 55.

(12) Teissié, J.; Prats, M.; Soucaille, P.; Tocanne, J. F. *Proc. Natl. Acad. Sci. U.S.A.* **1985**, *82*, 3217.

(13) Prats, M.; Teissié, J.; Tocanne, J. F. *Nature* **1986**, *322*, 756.

(14) Sakurai, I.; Kawamura, Y.; *Biochim. Biophys. Acta* **1987**, *904*, 405.

(15) Sakurai, I.; Kawamura, Y. *Biochim. Biophys. Acta* **1989**, *985*, 347.

(16) Morgan, H.; Taylor, D. M.; Oliverira, O. N. Jr. *Chem. Phys. Lett.* **1988**, *150*, 311.

(17) Morgan, H.; Taylor, D. M.; Oliverira, O. N. Jr. *Biochim. Biophys. Acta* **1991**, *1062*, 149.

(18) Nachliel, E.; Gutman, J. M. *Am. Chem. Soc*. **1988**, *110*, 2629.

(19) Gutman, M.; Nachliel, E.; Moshshiach, S. *Biochemistry* **1988**, *28*, 2936.

(20) Kasianowicz, J.; Benz, R.; McLaughlin, S. *J. Membr. Biol*. **1987**, *95*, 73.

(21) Menger, F. M.; Richardson, S. D.; Bromley, G. R. *J. Am. Chem. Soc*. **1989**, *111*, 6893.

(22) Chiou, J. S.; Krishna, P. R.; Kamaya, H.; Ueda, I. *Biochim. Biophys. Acta* **1992**, *1110*, 225.

(23) Shieh, D. D.; Ueda, I.; Lin, H. C.; Eyring, H. *Proc. Natl. Acad. Sci. U.S.A.* **1976**, *73*, 3999.

(24) Yokono, S.; Shieh, D. D.; Ueda, I. *Biochim. Biophys. Acta* **1981**, *645*, 237.

(25) Kamaya, H.; Kaneshina, S.; Ueda, I. *Biochim. Biophys. Acta* **1981**, *646*, 135.

(26) Kaneshina, S.; Kamaya, H.; Ueda, I. *J. Colloid Interface Sci*. **1983**, *93*, 215.